[Chem. Pharm. Bull. 32(3)1063—1070(1984)]

The Stability of Nicorandil in Aqueous Solution. I. Kinetics and Mechanism of Decomposition of *N*-(2-Hydroxyethyl)nicotinamide Nitrate (Ester) in Aqueous Solution

HIROSHI NAGAI,* MINEO KIKUCHI, HIROYUKI NAGANO and MOTOHARU SHIBA

Drug Development Laboratory, New Drug Research Laboratory, Chugai Pharmaceutical Co., Ltd., Toshima-ku, Takada 3–41–8, Tokyo 171, Japan

(Received May 12, 1983)

The extent and mechanism of decomposition of Nicorandil [*N*-(2-hydroxyethyl)nicotinamide nitrate (ester)] (I) in aqueous solution at various pH values were clarified. Four products derived from (I) were isolated and identified as 2-(3-pyridyl)-2-oxazoline (II), 2-aminoethyl nicotinate nitrate (III), *N*-(2-hydroxyethyl)nicotinamide (IV) and nicotinic acid (V). The decomposition products and (I) were quantitated by high performance liquid chromatography. The decompositions of (I), (II) and (III) followed pseudo first-order kinetics, while (IV) and (V) did not decompose further in the range of pH 4 to 11. Arrhenius plots of the rate constant for (I) were linear and the apparent activation energy for (I) was 25 kcal/mol at pH 7.0. The decomposition in aqueous solution was found to occur by a stepwise mechanism, with (I) cyclizing to form (II), which undergoes ring-opening to give (III), followed by competitive reactions, that is, rearrangement and hydrolysis, to form (IV) and (V) in the pH range of 4 to 11.

Keywords——Nicorandil; *N*-(2-hydroxyethyl)nicotinamide nitrate (ester); 2-(3-pyridyl)-2-oxazoline; 2-aminoethyl nicotinate nitrate; *N*-(2-hydroxyethyl)nicotinamide; nicotinic acid; HPLC; decomposition mechanism; reaction rate constant

By interacting with adjacent atoms, neighboring amide groups often facilitate solvolytic, oxidation-reduction and displacement reactions. For example, it is well known that *N*-2-bromoethyl benzamide and *N*-2-tosylethyl benzamide cyclize upon attack by oxygen to form 2-oxazoline,[1] and the facilitation of the cyclization by an electron-withdrawing group at the *p*-position of the phenyl group has been reported.[2] On the other hand, Zioudrou *et al.* reported that neighboring amide anions facilitate displacement of phosphate ester, chloride and tosylate from *p*-nitrobenzamide derivatives. The order of reactivity for the formation of oxazoline is $OTs > OPO(OAr)_2 > Cl$.[3]

Nicorandil [*N*-(2-hydroxyethyl)nicotinamide nitrate (ester)] has been found to be an effective drug in the treatment of coronary heart disease.[4] Thus, it is of interest to examine the behavior of Nicorandil with its pyridyl and nitrate groups, and to study the intramolecular cyclization and further decomposition processes. In this study, the reaction mechanism and kinetics of Nicorandil in buffer solution of various pH values were investigated.

Experimental

Apparatus——The infrared (IR) spectra were measured with a Hitachi model 285 spectrophotometer. The nuclear magnetic resonance (NMR) spectra were obtained in a JNM-FX 100 spectrometer using tetramethylsilane as an internal standard. Melting points were measured with a Mettler FP-5 FP-51 auto melting point apparatus and pH with a Toa HM-20B pH meter. The mass spectra (MS) were obtained using a Shimadzu LKB-9000 instrument. The ultraviolet (UV) spectra were obtained with a Hitachi model 320 spectrophotometer. High performance liquid chromatography (HPLC) was done on a Waters liquid chromatograph (model ALC/GPC 244) with a UV absorbance detector (model 440) operating at 254 nm and a 300 × 3.9 mm i.d. column packed with μ-Bondapak C_{18}.

Other conditions were as follows: eluent, 0.01 M $(NH_4)_2$ HPO_4 (pH 7.5) containing MeOH (30%); flow rate, 2 ml/min. Peak areas were determined with a Shimadzu Chromatopak E-1B. Thin layer chromatograms (TLC) were run on Merck silica gel 60 F_{254} precoated plates using *n*-PrOH : 10% ammonia water = 9 : 1 (solvent A), *n*-BuOH : AcOH : water = 4 : 1 : 1 (solvent B) and acetone (solvent C) as developers, and were observed under UV light (main wavelength 254 nm).

Reagents——All the reagents mentioned were of analytical reagent grade.

Preparation of Materials——(i) Nicorandil: Nicorandil was synthesized according to Japanese patent 122373 (1977).

(ii) 2-(3-Pyridyl)-2-oxazoline: Nicorandil (100 mg) was dissolved in 0.1 N NaOH (100 ml) and the solution was maintained at 60 °C for 300 min. After cooling, the solution was extracted with $CHCl_3$ (50 ml) three times. The extract was washed with water and evaporated to dryness under reduced pressure to give a white powder. Recrystallization from $CHCl_3$–hexane gave white needles (60 mg). mp 69.9 °C (lit. 71 °C)[5] *Anal.* Calcd for $C_8H_8N_2O$: C, 64.69; H, 5.44; N, 18.91. Found: C, 64.69; H, 5.46; N, 18.82. UV $\lambda_{max}^{H_2O}$ 242 nm. IR (KBr): 1655 ($\nu_{C=N}$), 1075 (ν_{C-O-C}) cm^{-1}. ^{1}H-NMR (3% solution in DMSO-d_6) δ: 4.0, 4.4 (O–C$\underline{H}_2$C$\underline{H}_2$). MS *m/e*: 148 (M^+).

(iii) 2-Aminoethyl Nicotinate Nitrate: Nicorandil (100 mg) was dissolved in water (10 ml) and the solution was maintained at 70 °C for 240 min, then cooled. Iso-PrOH was added to the solution to give a white powder. Recrystallization from water–MeOH gave white crystals (40 mg). mp 150.0 °C, *Anal.* Calcd for $C_8H_{11}N_3O_5$: C, 41.93; H, 4.83; N, 18.33. Found: C, 41.77; H, 4.89; N, 18.18. UV $\lambda_{max}^{H_2O}$ 263 nm. IR (KBr): 1715 ($\nu_{C=O}$), 1382 ($\nu_{NO_3^-}$), 1125 (ν_{C-O-C}) cm^{-1}. ^{1}H-NMR (3% solution in DMSO-d_6) δ: 4.5 (O–C$\underline{H}_2$), 3.3 (C$\underline{H}_2$–N), 8.1 (N$\underline{H}_2$). MS *m/e*: 167 ($M^+ - NO_3$).

(iv) *N*-(2-Hydroxyethyl)nicotinamide: This compound was synthesized according to Drefahl *et al.*[5] mp 90.2 °C, *Anal.* Calcd for $C_8H_{10}N_2O_2$: C, 57.82; H, 6.07; N, 16.86. Found: C, 57.88; H, 6.09; N, 16.85. UV $\lambda_{max}^{H_2O}$ 261 nm. IR (KBr): 1665 ($\nu_{C=O}$), 1545 (δ_{NH}), 1295 (ν_{C-N}) cm^{-1}. ^{1}H-NMR (3% solution in DMSO-d_6) δ: 8.7 (N$\underline{H}$), 3.4 (N–C$\underline{H}_2$C$\underline{H}_2$), 4.8 (O$\underline{H}$). MS *m/e*: 166 (M^+), 135 ($M^+ - CH_2OH$), 106 ($M^+ - NHCH_2CH_2OH$), 78 ($M^+ - CONHCH_2CH_2OH$).

Identification of Decomposition Products——Nicorandil (100 mg) was dissolved in pH 4.0, 7.0 and 9.0 buffers, described below, and the solution was maintained at 60 °C for 420 min. Then 10 μl aliquots of buffer solution were applied to the TLC plates, developed with three solvent systems and detected under UV light at 254 nm. In the sample stored at pH 7.0, three new spots, (II), (III) and (IV) were noted. The *Rf* values of (II), (III) and (IV) were the same as those of authentic 2-(3-pyridyl)-2-oxazoline, 2-aminoethyl nicotinate nitrate and *N*-(2-hydroxyethyl)nicotinamide, respectively, in three different solvent systems. *Rf*: (II), 0.44 (solvent A), 0.43 (solvent B), 0.30 (solvent C); (III), 0.40 (solvent A), 0.25 (solvent B), 0.09 (solvent C); (IV), 0.38 (solvent A), 0.38 (solvent B), 0.19 (solvent C).

At pH 4.0, (III) and a new spot (V) were detected. The *Rf* value of (V) was the same as that of authentic nicotinic acid in three different solvent systems. *Rf*: (V), 0.25 (solvent A), 0.38 (solvent B), 0.11 (solvent C).

At pH 9.0, (II) and (IV) were also detected on the TLC plates.

Kinetics——Buffers employed were 0.1, 0.2 or 0.3 M AcONa–AcOH (pH 4.0—5.0), 0.1, 0.2 or 0.3 M Na_2HPO_4–NaH_2PO_4 (pH 6.0—8.0) and 0.1, 0.2 or 0.3 M Na_2CO_3–$NaHCO_3$ (pH 9.0—11.0). Ionic strength was maintained at 0.7 with KCl.

Nicorandil (I), 2-(3-pyridyl)-2-oxazoline (II), 2-aminoethyl nicotinate nitrate (III), *N*-(2-hydroxyethyl)-nicotinamide (IV) and nicotinic acid (V) dissolved in each buffer at a concentration of 5×10^{-3} M were stored at 40, 50 or 60 °C and samples (1.0 ml) were taken at intervals. To 1.0 ml of each aliquot, 1.0 ml of internal standard solution (0.1% 2,4-dinitrochlorobenzene in MeOH) was added, together with water to make exactly 25 ml, and a 15 μl aliquot was injected onto the HPLC column. The concentration of each compound was calculated by the use of a calibration curve. The coefficient of variation of the assay was 1.5—2.4% for each compound.

Results and Discussion

After storage of (I) in pH 4.0, 7.0 and 9.0 buffers at 60 °C for 420 min, four new spots were observed on TLC plates. (II) was identified as 2-(3-pyridyl)-2-oxazoline, (III) was identified as 2-aminoethyl nicotinate nitrate, (IV) as *N*-(2-hydroxyethyl)nicotinamide and (V) as nicotinic acid. Under these conditions, upon further heating for a period of approximately 600000 min, (IV) and (V) were formed gradually and no new products were detected. This means that the decomposition process is terminated by the formation of (IV) and (V). For determining the reaction rates in this decomposition reaction system in detail, the HPLC method mentioned above was the most suitable because all the products could be determined simultaneously. Typical chromatograms are shown in Fig. 1.

The result for (I) (pH 7.0, 60 °C) obtained by HPLC is shown in Fig. 2. As time passed,

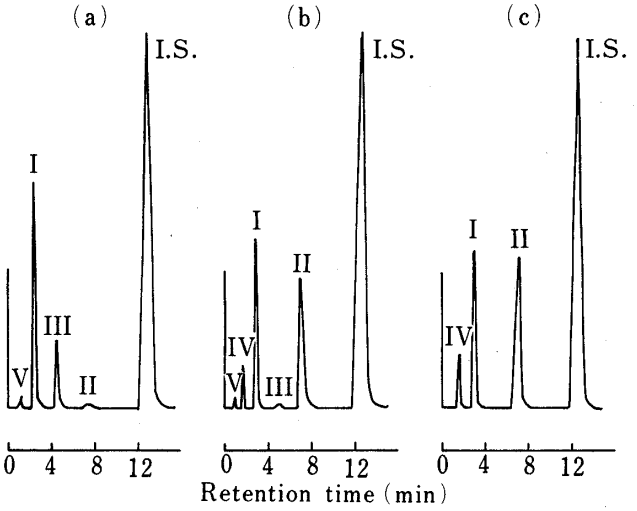

Fig. 1. Chromatograms of Aqueous Solutions of (I) Obtained by HPLC

a) 0.1 M acetate buffer, pH 4.0 after 360 min at 60 °C.
b) 0.1 M phosphate buffer, pH 7.0 after 360 min at 60 °C.
c) 0.1 M carbonate buffer, pH 9.0 after 360 min at 60 °C.

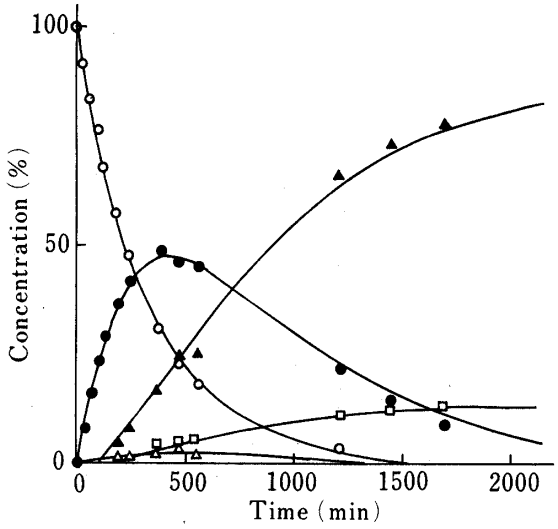

Fig. 2. Time Courses of (I) (○), (II) (●), (III) (△), (IV) (▲) and (V) (□) during the Decomposition of (I) in 0.1 M Phosphate Buffer, pH 7.0, at 60 °C

The solid lines are calculated values based on Eqs. (1), (2), (3), (4) and (5).

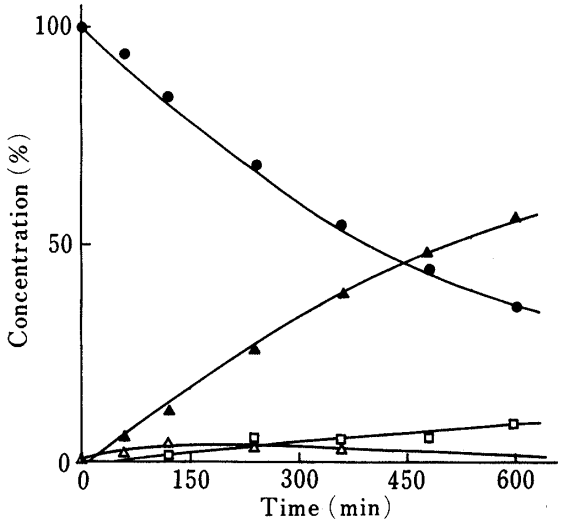

Fig. 3. Time Courses of (II) (●), (III) (△), (IV) (▲) and (V) (□) during the Decomposition of (II) in 0.1 M Phosphate Buffer, pH 7.0, at 60 °C

The solid lines are calculated values.

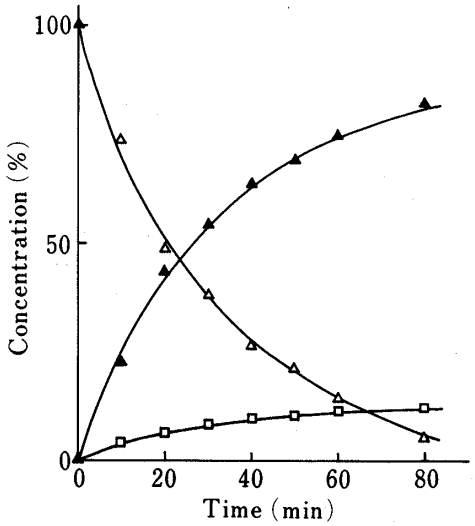

Fig. 4. Time Courses of (III) (△), (IV) (▲) and (V) (□) during the Decomposition of (III) in 0.1 M Phosphate Buffer, pH 7.0, at 60 °C

The solid lines are calculated values.

(I) decreased rapidly, (II) and (III) reached maxima after 360 and 480 min, respectively, and finally (IV) and (V) were formed gradually with a lag time. The behavior of (II) and (III) under the same conditions is shown in Figs. 3 and 4.

As can be seen in Fig. 3, (II) decomposed and after 90 min (III) reached a maximum, while (IV) and (V) were formed in the same manner as in the case of (I). In the case of (III), (III) decreased and (IV) and (V) were formed. These results suggest that the decomposition reaction of (I) follows the successive reaction mechanism shown in Chart 1.

The apparent rate constants, k_1, k_2, k_3 and k_4, shown in Chart 1 were determined independently as follows. As the relationship between reaction time and the logarithm of the

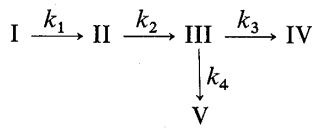

Chart 1

TABLE I. Rate Constant for Each Reaction Route at 60 °C and Ionic Strength 0.7

pH	k_1 (min^{-1})	k_2 (min^{-1})	k_3 (min^{-1})	k_4 (min^{-1})
4.0	2.45×10^{-3}	7.87×10^{-2}	4.74×10^{-6}	6.77×10^{-5}
5.0	2.79×10^{-3}	9.08×10^{-3}	3.70×10^{-5}	1.29×10^{-4}
6.0	2.87×10^{-3}	4.42×10^{-3}	6.59×10^{-4}	4.61×10^{-4}
7.0	2.78×10^{-3}	1.72×10^{-3}	3.36×10^{-2}	4.94×10^{-3}
8.0	2.84×10^{-3}	8.45×10^{-4}	2.32×10^{-1}	1.27×10^{-2}
9.0	3.24×10^{-3}	8.10×10^{-4}	1.39	1.44×10^{-2}
10.0	4.15×10^{-3}	7.18×10^{-4}	7.19	9.80×10^{-2}
11.0	1.20×10^{-2}	7.01×10^{-4}	1.10×10	2.10×10^{-1}

concentration of residual (I) showed good linearity under all conditions, this reaction was regarded as a pseudo first-order reaction. In the cases of (II) and (III), the relation between reaction time and the logarithm of the concentration of each compound also showed good linearity and these reactions were thus also psuedo first-order. The rate constants, k_1 and k_2 were therefore determined from the decrease of (I) or (II), respectively. The values of k_3 and k_4 were calculated from the obtained values of (IV) and (V) during the decomposition of (III). The rate constants in 0.1 M buffers at 60 °C are collected in Table I; these values did not vary when the initial concentrations were ten times higher or one-tenth as much.

When (I) was heated at a given temperature, the concentration of each reactant at a time t can be represented as follows. In these equations, a is the concentration of (I) at time 0.

$$[\mathrm{I}] = a\exp(-k_1t) \tag{1}$$

$$[\mathrm{II}] = ak_1/(k_2-k_1)\,[\exp(-k_1t)-\exp(-k_2t)] \tag{2}$$

$$[\mathrm{III}] = ak_1k_2/(k_2-k_1)(k_3+k_4-k_1)\exp(-k_1t)-ak_1k_2/(k_2-k_1)(k_3+k_4-k_2)\exp(-k_2t)+ak_1k_2/(k_3+k_4-k_1)(k_3+k_4-k_2)\exp[-(k_3+k_4)t] \tag{3}$$

$$[\mathrm{IV}] = ak_3/(k_3+k_4)-ak_2k_3/(k_2-k_1)(k_3+k_4-k_1)\exp(-k_1t)+ak_1k_3/(k_2-k_1)(k_3+k_4-k_2)\exp(-k_2t)-ak_1k_2k_3/(k_3+k_4-k_1)(k_3+k_4-k_2)(k_3+k_4)\exp[-(k_3+k_4)t] \tag{4}$$

$$[\mathrm{V}] = ak_4/(k_3+k_4)-ak_2k_4/(k_2-k_1)(k_3+k_4-k_1)\exp(-k_1t)+ak_1k_4/(k_2-k_1)(k_3+k_4-k_2)\exp(-k_2t)-ak_1k_2k_4/(k_3+k_4-k_1)(k_3+k_4-k_2)(k_3+k_4)\exp[-(k_3+k_4)t] \tag{5}$$

The time courses of (I) and its decomposition products during the decomposition of (I) at pH 4.0, 7.0 and 9.0 are shown in Figs. 2, 5 and 6.

Solid lines indicate the calculated curves evaluated according to Eqs. (1), (2), (3), (4) and

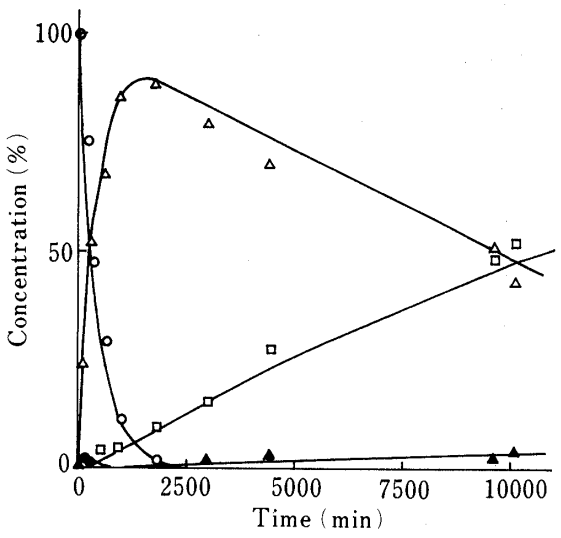

Fig. 5. Time Courses of (I) (○), (II) (●), (III) (△), (IV) (▲) and (V) (□) during the Decomposition of (I) in 0.1 M Acetate Buffer, pH 4.0, at 60 °C

The solid lines are calculated values based on Eqs. (1), (2), (3), (4) and (5).

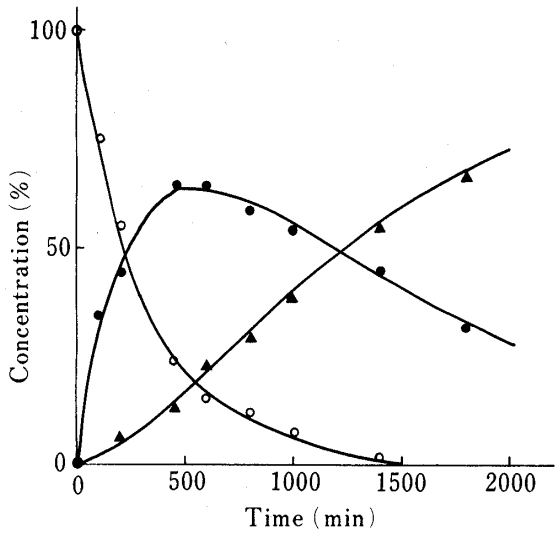

Fig. 6. Time Courses of (I) (○), (II) (●), (III) (△), (IV) (▲) and (V) (□) during the Decomposition of (I) in 0.1 M Carbonate Buffer, pH 9.0, at 60 °C

The solid lines are calculated values based on Eqs. (1), (2), (3), (4) and (5).

TABLE II. Activation Energy of Each Reaction Step at pH 7.0

Reaction step	E_a (kcal/mol)
(I)→(II)	25.1
(II)→(III)	15.1
(III)→(IV)	27.7
(III)→(V)	27.7

(5). In these equations, each rate constant k_1, k_2, k_3 and k_4 was independently determined from the reactions of (I), (II) and (III) described above. Figures 2, 5 and 6 show the observed concentrations of (I), (II), (III), (IV) and (V) during the decomposition of (I). These values agree very closely with the calculated curves for each decomposition product. These results indicate that the presumed reaction pathway shown in Chart 1 is correct and that no other reaction occurs. Similar agreements between the calculated and observed values were obtained in the pH range of 4 to 11. The effect of temperature on k_1, k_2, k_3 and k_4 was determined at pH 7.0 at three different temperatures. The resulting Arrhenius plot was linear and the activation energy is shown in Table II.

Plots of log k *versus* pH at 60 °C are shown in Fig. 7.

In the first step of the reaction of (I), (I) is cyclized to (II) by attack of oxygen, but (IV), which is similar in structure to (I), did not undergo cyclization under these reaction conditions. It was found that k_1 did not vary between pH 4 and 8, but above pH 9, it increased with increasing pH. On the other hand, at a fixed pH and ionic strength, buffer concentration had no influence on the reaction rate constant k_1, as shown in Fig. 8.

Thus, two mechanisms can be postulated. In the basic region, rapid reversible transfer of a proton between the N–H group of the amide and a hydroxide ion followed by the displacement of the nitrate ion occurs. In the neutral region between pH 4 and 8, cyclization probably involves attack by the neutral form of the neighboring group. The center of nucleophilicity of the amide, the oxygen atom attacks the β-carbon, which is polarized

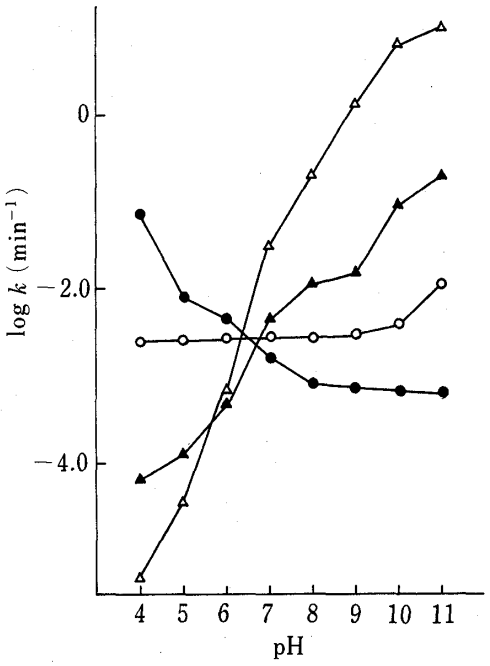

Fig. 7. pH-Rate Profiles for the Decomposition of (I), (II) and (III) in 0.1 M Buffers at 60 °C
○, k_1; ●, k_2; △, k_3; ▲, k_4.

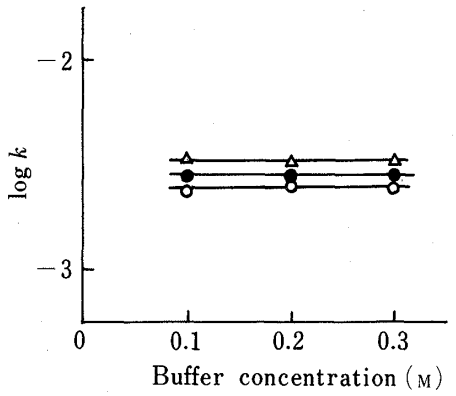

Fig. 8. Effect of Buffer Concentration on the Pseudo First-Order Rate Constant k_1
○, pH 4.0; ●, pH 7.0; △, pH 9.0.
All the runs were carried out at 60 °C and ionic strength 0.7.

because of the strong electron-withdrawing property of the nitrate moiety of (I). At pH 11, cyclization was 4 times faster than in the neutral region. It appears that the nucleophilicity of the conjugated amide group is stronger than that of the neutral amide. This tendency is consistent with Heine's results[2] (Chart 2).

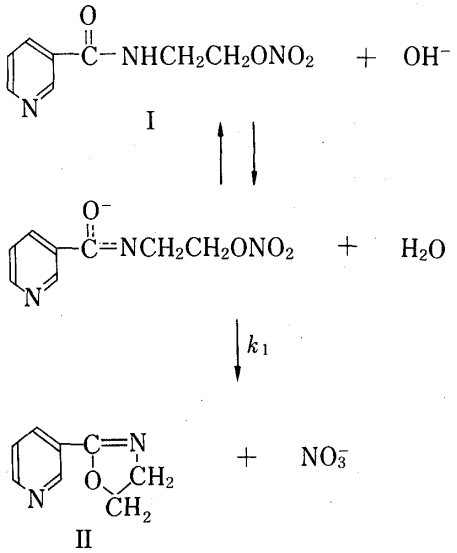

Chart 2

As the pH in the range from 4 to 8 is increased, the rate constant for the reaction of (II) decreases. The slope of the plot for k_2 was (−1) in the range between pH 4 and 5 as shown in Fig. 7. The rate constant at pH 4 was 110 times larger than that at pH 11. From these results, it seems reasonable to assume the formation of the oxazoline cation (IIb), which is hydrolyzed to form (III); the concentration of the intermediate (IIb) is the rate-limiting factor (Chart 3).

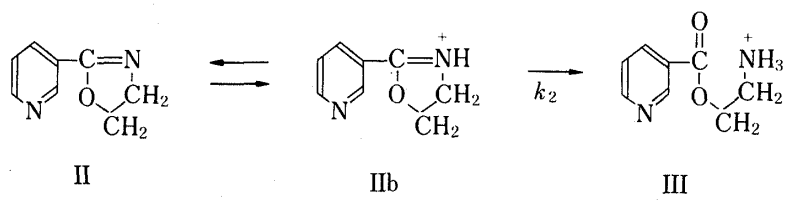

II IIb III

Chart 3

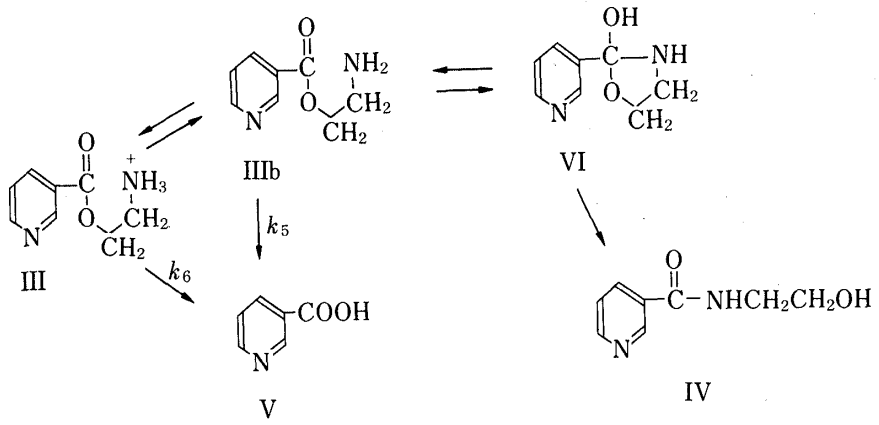

III IIIb V VI IV

Chart 4

In contrast with k_2, k_3 and k_4 increased with increasing pH; k_3 at pH 11 was 2×10^6 times larger than at pH 4, and the formation of (IV) was the main reaction in the alkaline region. The formation of (IV) from (III) is an intramolecular aminolysis reaction. It is well known that the aminolysis of esters proceeds *via* unstable tetrahedral addition intermediates. In the case of intramolecular aminolysis, a similar cyclic addition intermediate can also be considered. We have now shown that the rate-determining step of intramolecular aminolysis changes with change of pH. At low pH, breakdown of the cyclic intermediate is the rate-determining step, while at high pH the formation of the cyclic intermediate is the rate-determining step.[6] In the decomposition of (III) it is considered that the reaction proceeds in the same way.

As regards the formation of (V), it is considered that k_4 is the sum of two reaction constants, k_5 and k_6. The contribution of these constants to k_4 depends upon pH. However, it is not possible to explain the mechanism of the hydrolysis of (III) in detail only from the log k *vs.* pH profile.

On the other hand, it was observed that tertiary 2-ammoniumethyl acetates were hydrolyzed more rapidly than quaternary esters owing to intramolecular hydrogen bond catalysis; this hydrogen bonding increased the positive charge of the carbon atom, which is thus more easily attacked by a hydroxide ion.[7] The rate constant of alkaline hydrolysis for 2-dimethylaminoethyl acetate is ten times larger than k_4 at pH 7.0 at 25 °C.[8] It is difficult to explain the small value for (III) as compared with other 2-aminoalkyl esters. As the hydrogen bond of (III) is presumably broken more easily than those of 2-aminoalkyl esters because there are three protons, the formation of (IV) may proceed faster. This may account in part for the small k_4. In the acidic region, (III)→(V) is the main pathway because [IIIb] is smaller than [III] (Chart 4).

Acknowledgement The authors are grateful to Dr. S. Tominaga, director of the laboratory, for permission to publish this work. Thanks are also due to the members of this division for their encouragement and helpful suggestions.

References and Notes

1) F. L. Scott, R. E. Glick and S. Winstein, *Experientia*, **13**, 183 (1953).
2) H. W. Heine, *J. Am. Chem. Soc.*, **78**, 3708 (1956).
3) C. Zioudrou and G. L. Schmir, *J. Am. Chem. Soc.*, **85**, 3258 (1963).
4) Y. Uchida, N. Yoshimoto and S. Murao, *Jpn. Heart J.*, **19**, 112 (1978); Y. Nakagawa, K. Takeda, Y. Katano, T. Tsukada, T. Kitagawa and T. Otorii, *ibid.*, **20**, 881 (1979); Y. Uchida, *Saishin Igaku*, **33**, 1629 (1978).
5) G. Drefahl and K. König, *Chem. Ber.*, **87**, 1268 (1954).
6) M. L. Bender, *Chem. Rev.*, **60**, 53 (1960); B. Hansen, *Acta Chem. Scand.*, **17**, 1307 (1963); G. M. Blackburn and W. P. Jencks, *J. Am. Chem. Soc.*, **90**, 2638 (1968); G. L. Schmir, *ibid.*, **90**, 3478 (1968); A. C. Satterthwait and W. P. Jencks, *ibid.*, **96**, 7018 (1974); M. Caswell, R. K. Chaturvedi, S. M. Lane, B. Zivilicovsky and G. L. Schmir, *J. Org. Chem.*, **46**, 1585 (1981).
7) A. Ägren, U. Hedsten and B. Josson, *Acta Chem. Scand.*, **15**, 1532 (1961); B. Hansen, *ibid.*, **16**, 1927 (1962); K. Kigasawa and H. Ohtani, *Yakugaku Zasshi*, **95**, 1405 (1975).
8) k_4 at pH 7.0 and 25°C was obtained from the Arrhenius equation.